

Received May 8, 2019, accepted June 6, 2019, date of publication July 15, 2019, date of current version August 7, 2019.

Digital Object Identifier 10.1109/ACCESS.2019.2928944

DC-Bias for Optical OFDM in Visible Light Communications

XIONG DENG^{1,2}, (Member, IEEE), SHOKOUFEH MARDANIKORANI²,
GUOFU ZHOU¹, AND JEAN-PAUL M. G. LINNARTZ^{2,3}, (Fellow, IEEE)

¹National Center for International Research on Green Optoelectronics, South China Normal University, Guangzhou 510006 China

²Department of Electrical Engineering, Eindhoven University of Technology, 5600 MB Eindhoven, The Netherlands

³Signify (Philips Lighting) Research, 5656 AE Eindhoven, The Netherlands

Corresponding author: Shokoufeh Mardanikorani (S.Mardanikorani@tue.nl)

ABSTRACT The requirement of a DC-bias is known to make DC-biased optical orthogonal frequency division multiplexing (DCO-OFDM) less energy efficient. This can be improved by asymmetrically clipped optical OFDM (ACO-OFDM), pulse amplitude modulated OFDM (PAM-OFDM) or Flip-OFDM, but these variants use the bandwidth inefficiently. Our trade-off between energy and spectrum efficiency considers a given limited channel bandwidth of the light emitting diode (LED) and then attempts to get the highest throughput per unit of energy. We investigate previous findings that clipped OFDM can be more attractive in a low-SNR regime. More specifically, we consider visible light communication (VLC) in which the average light level, i.e., the bias, is prescribed by illumination requirements, thus comes for free. ACO/PAM/Flip-OFDM can convert the DC-bias into power for communication, but all variants of OFDM, including DCO-OFDM consume extra electrical power. We conclude that in this scenario, advantages attributed to ACO/PAM/Flip-OFDM vanish, as DCO-OFDM outperforms its variants in all SNR conditions, in terms of achieved throughput over a bandlimited channel as a function of extra electrical power required. For hybrid solutions, such as Asymmetrically clipped DC biased Optical OFDM (ADO-OFDM) and Hybrid ACO-OFDM (HACO-OFDM), we optimize a new adaptive power and rate splitting between odd (clipped) and even (biased/clipped) subcarriers to balance power and bandwidth efficiency.

INDEX TERMS Illumination, communication, VLC, capacity, DC bias, OFDM.

I. INTRODUCTION

Orthogonal Frequency Division Multiplexing (OFDM) is widely considered as a modulation technique for an Intensity Modulated/Direct Detection (IM/DD) optical wireless system, because of its ability to transform the full bandwidth channel into smaller subchannels, each with a flat response within their subband. It can avoid Inter Symbol Interference (ISI) and thus provides resistance to dispersive channel. A simple one-tap equalizer at the receiver can be used and the adaptive, frequency-dependent power and (or) bit loading can be applied. OFDM is proposed for Optical Wireless Communication (OWC) in the ITU-T G.9991 (g.vlc), the IEEE 802.15.7m and the IEEE 802.11bb and other standards.

In IM/DD optical system, the intensity of light can neither be complex nor negative. Thus, the input feeding the Inverse Fast Fourier Transform (IFFT) during the OFDM

generation flow is constrained to have an Hermitian symmetry to deliver a real-valued signal, then a DC-bias is usually applied to ensure a positive output, called DC-biased Optical OFDM (DCO-OFDM) [1]–[3]. The main idea for Asymmetrically Clipped Optical OFDM (ACO-OFDM), Pulse Amplitude Modulated OFDM (PAM-OFDM) or Flip OFDM is to avoid the power inefficient DC bias so as to improve the energy efficiency [4]–[7]. To be specific, ACO/Flip/PAM-OFDM effectively convert and re-utilize the power “wasted” in a DC-bias into a power that carries signal data. This comes at a price in bandwidth utilization, as in ACO/Flip/PAM-OFDM only half of the signal dimensions effectively carry data [8]. This puts a 50% penalty on the capacity. To repair the spectrum efficiency, Asymmetrically clipped DC biased Optical OFDM (ADO-OFDM) [5] transmits ACO-OFDM on the odd subcarriers and adds DCO-OFDM on the even subcarriers. Hybrid ACO-OFDM (HACO-OFDM) simultaneously uses ACO-OFDM on odd subcarriers and PAM-DMT on even subcarriers [9].

The associate editor coordinating the review of this manuscript and approving it for publication was Wei Xu.

The energy efficiency (in bits/s/J) is an appropriate metric if power is limited but bandwidth is unlimited [10], [11]. The spectrum efficiency (in bits/s/Hz) is appropriate if power is for free but bandwidth is scarce. Yet in practice, both power and bandwidth are constrained. This has been addressed by plotting the power and bandwidth efficiency on different axes to map various modulation schemes. In this paper, we take the position that the channel bandwidth often is a hard constraint [12], [13], while our design objective is to get the highest possible bit rate for a given power budget. This calls for an optimization of the maximum throughput per available dimension, as a function of the link budget. To this end, we invoke the Shannon channel capacity expression and compare various methods not only based on the same optical signal power, but in particular analyze and compare this for the electrical power fed into the Light Emitting Diode (LED).

Depending on whether we compare a system based on optical or electrical power, one can arrive at different conclusions. In fact, the optical power constrains the first moment (the mean) of the LED current, while the total and extra electrical power constrain the second moment and the variance (central moment), respectively. If eye-safety is the prime limitation, optical power may be an appropriate comparison [5]. It has been revealed that modulating a constant illumination light level costs extra electrical power, while the time-average optical power remains constant [14]. As the power consumption in mobile devices is limited, the *electrical power* consumed in the LED or in the driver is more appropriate, while this was less commonly studied in literature and we will focus on this aspect.

For Infrared (IR) communication, the second moment (variance plus square of the mean, including bias) determines the electrical power in the LED, while for the Power Amplifier (PA) also the Peak-to-Average Power Ratio (PAPR) is relevant. Thus, a comparison purely based on average optical power (first moment of the photonic flux) oversimplifies. This paper, we revisit some results by extending this model. Yet for Visible Light Communication (VLC), where illumination constraints already give a DC bias for free, the *extra electrical power* consumed with respect to unmodulated illumination is more relevant. Intuitively, it seems that the system that excels on the basis of total power will also excel if benchmarked on extra power. Nevertheless in this paper we challenge this thought. As we will see, for DCO-OFDM with a given DC lighting setting, one can use arbitrary amounts of extra power to communicate, including very small modulation depths that do not affect the overall energy efficiency of the light source. In fact, anticipating on results in Section IV, with ACO/Flip/PAM-OFDM, the extra power for modulation can, depending on the LED and its operation, be significantly above 20% of the illumination only power. This would severely deteriorate the efficiency of LED lighting and may disqualify its energy star compliance [15]. We see that different conclusions apply for VLC and IR communication, particular if VLC is positioned as an increment to a prime illumination function.

Comparisons from other perspectives than we focus on in this paper include, for instance, PAPR and nonlinearity tolerance which are relevant to practical implementation. Assuming the same power after IFFT, the ACO/Flip/PAM-OFDM PAPR is 6.9 dB higher than the DCO-OFDM PAPR, due to the halved power after the clipping or flipping. For the impact of the PAPR on the extra power lost in the LED modulator, we refer to [16]. Secondly, LED nonlinearities tend to be smaller at the center of the dynamic range and are higher at the edges. Since ACO/Flip/PAM-OFDM has higher sample density close to the lower part of the dynamic range, it will be more affected by nonlinearities which will increase the BER. We know from [13] that nonlinearities cannot be eliminated with a static separate predistorter, but requires a non-linear equalizer with non-linear delay taps, which raises the question whether in addition, the frequency domain equalisation in OFDM is still attractive or needed.

In this study, we compare the performance of optical OFDM variants with (extra) electrical power or energy employing Shannon channel capacity. The rest of the paper is organized as follows. Section II describes the linearized LED model and typical VLC channel. DCO-OFDM is presented in Section III. ACO-OFDM, Flip-OFDM and PAM-OFDM are discussed in Section IV. The performance of the improved ADO-OFDM and HACO-OFDM are presented in Section V. Performance evaluation and comparison is discussed in Section VI. Conclusions are drawn in Section VII.

II. LED AND VLC CHANNEL

This section discusses in more detail on LED model and VLC channel, which forms the basis for the modeling of power efficiency throughout this paper.

A. LINEARIZED LED MODEL

The voltage across the LED V_{LED} is a function of the current through the LED I_{LED} , described by

$$V_{LED} = \frac{nkT}{q} \ln \left[\frac{I_{LED}}{I_s} + 1 \right] + R_L I_{LED}, \quad (1)$$

where n is the ideality factor ($n = 1$ to 2), k is the Boltzmann constant, T is the temperature in Kelvin, q is the electron charge. At room temperature, $kT/q = 26$ mV. The saturation current I_s highly depends on the LED type, where a typical example is $I_s = 4.1 \times 10^{-24}$ A with $n = 1.4$ [17]. Above a few milliamps, the DC resistance R_L in the LED needs to be considered.

We linearize the LED model as a fixed junction voltage V_J in series with a dynamic and Equivalent Series Resistance (ESR) resistance R_{LED} [16]. Thus,

$$V_{LED} = V_J + I_{LED} R_{LED}, \quad (2)$$

where V_J is not the voltage at which the dynamic resistance is obtained, but the crossing point of the linearized LED mode with the horizontal axis ($I_{LED} = 0$). Fig. 1 shows a typical LED I-V curve and the linearization approximation, which

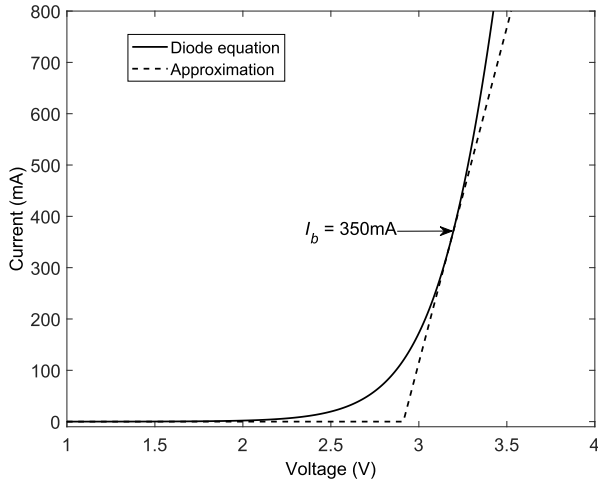


FIGURE 1. A typical LED V-I curve using the diode equation from Eq. (1) (solid line) and linear approximation from Eq. (2) (dashed line).

confirms that for a small modulation in current, the linearization is reasonable.

The photon light generation $\phi(t)$ of the LED is proportional to the driving current $I_{LED}(t)$, with $\phi(t) = aI_{LED}(t)$, where a is called the LED responsivity in W/A.

B. VLC CHANNEL MODEL

OWC system over an optical IM/DD channel is typically modeled as a baseband linear system with the optical signal $\phi(t)$ transmitted over a channel with equivalent impulse response $h(t)$, which leads to an received current $r(t)$ with an additive Gaussian noise $n(t)$ [18], [19]. The received signal is expressed as the convolution

$$r(t) = b\phi(t) \otimes h(t) + n(t), \quad (3)$$

where b is the responsivity (A/W) of the photodetector (PD). For a detailed analysis of the impact of $h(t)$ or rather its frequency transfer function $H(f)$ on the capacity, we refer to [20]. Our analysis here can be seen as an optimization that focuses on the modulation of the OFDM subcarriers within a flat portion of the received spectrum, while [20] focuses on the trade-off between subcarriers.

The path from an LED to a PD is usually modeled as a flat channel with a fixed propagation delay and DC gain. Multipath frequency selectivity can play a role, but only for high modulation rates. Most papers copy the Lambertian radiation expression [18], [21], [22], but lighting systems mostly have dedicated optics to optimize illumination, it may not generically apply [23], [24]. As our findings do not in any way depend on the radiation pattern, we collapse the emission pattern and path loss into a single h_0 that denotes the optical channel DC gain. The Gaussian noise $n(t)$ includes the shot noise and thermal noise [25], which both have a flat Power Spectrum Density (PSD) of

$$N_0 = N_{shot} + N_{thermal} = 2qbP_n + \frac{4kT}{R_F}, \quad (4)$$

where P_n and R_F are the received optical power at the PD and feedback resistor of the Trans-Impedance Amplifier (TIA) in the receiver, respectively.

III. DCO-OFDM

Since the optical power is the average light output, modulating the light intensity around an average illumination level does not imply extra optical power. Yet, when considering the electrical power, variations around an average light level cost significant amounts of extra energy, which we quantify here. In DCO-OFDM, a real-valued DC-free OFDM signal $i(t)$ is added to a DC bias I_{LED} , to generate the LED current $I_{LED}(t) = I_{LED} + i(t)$. If the number of subcarriers is large enough, the current acts as a Gaussian variable, with mean I_{LED} and standard deviation i_{rms} , where we denote the rms modulating OFDM current as $i_{rms} = \sqrt{\mathbb{E}[i^2(t)]}$. Using the linearized model, the power consumed in the LED is

$$\begin{aligned} \mathbb{E}[V_{LED}I_{LED}] &= V_J I_{LED} + R_{LED} \mathbb{E}[I_{LED} + i(t)]^2 \\ &= V_J I_{LED} + R_{LED} I_{LED}^2 + R_{LED} i_{rms}^2. \end{aligned} \quad (5)$$

We checked that for modulation below $i(t) < 0.3I_{LED}$, the accuracy of (5) is better than 0.3%. We assume that the DC bias is chosen such that the clipping artefacts can be neglected, then the optical power is equal to the DC bias I_{LED} [26]. For an underclipped OFDM, detailed calculation on the clipping noise can be found elsewhere [11], [27].

The modulating current is also expressed as $i(t) = \alpha(t)I_{LED}$, where the modulation $\alpha(t)$ is normalized to the LED DC current I_{LED} with $-1 \leq \alpha(t) \leq 1$. Thus the extra electrical power, relative to unmodulated illumination is $P_{\Delta DCO} = R_{LED} i_{rms}^2 = R_{LED} \alpha_{rms}^2 I_{LED}^2$, thus, it is a function of the root-mean-square modulation index $\alpha_{rms} = \sqrt{\mathbb{E}[\alpha^2(t)]}$, which is equivalent to the square root of the ratio of the AC power over the DC power. Fig. 2 gives a graphical interpretation of this mechanism behind the extra power loss in the LED for DCO-OFDM. In later sections, we want to express the received Signal Noise Ratio (SNR) as a function of the extra power spent at the transmitter. If we include the DC bias, the ratio of the power that effectively contributes to the SNR over the total consumed power is

$$\begin{aligned} \eta &= \frac{P_{\Delta DCO}}{P_{bias} + P_{\Delta DCO}} \\ &= \frac{R_{LED} \alpha_{rms}^2 I_{LED}^2}{V_J I_{LED} + R_{LED} (1 + \alpha_{rms}^2) I_{LED}^2}. \end{aligned} \quad (6)$$

It results in a received SNR of

$$SNR_{DCO} = \frac{P_{RX} T_s}{N_0} = \frac{a^2 b^2 T_s}{N_0} \alpha_{rms}^2 I_{LED}^2, \quad (7)$$

where the equivalent bandwidth $1/T_s$ is derived from the symbol rate [28]. For VLC, where illumination is needed anyhow, we take this SNR from extra power as a benchmark. For reference we define the normalized SNR

$$\gamma_{DCO} = \frac{a^2 b^2 T_s}{N_0 R_{LED}} P_{\Delta DCO}. \quad (8)$$

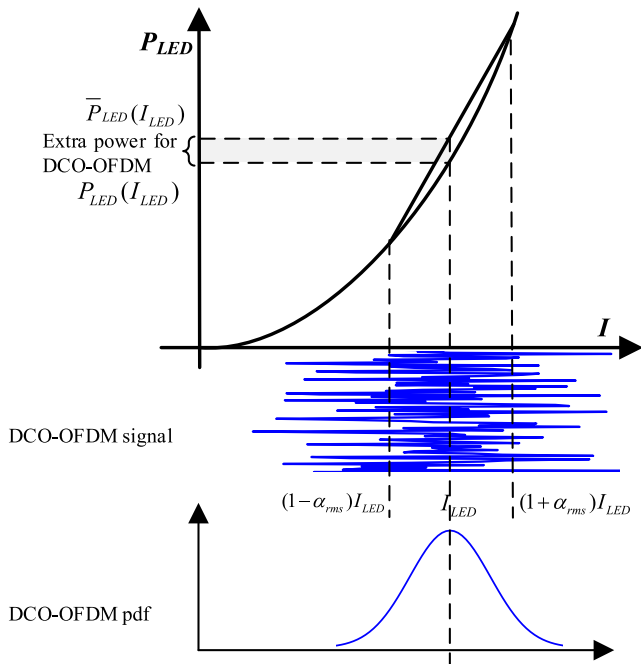


FIGURE 2. Explanation of the extra power loss in the LED for DCO-OFDM. Convex consumed electrical power versus current.

A. DCO-OFDM IN IR

For the case of IR communications, where the bias only serves to carry the data signal, it is more useful to express the channel capacity as a function of total consumed power P_{DCO} , thus including the DC bias power. This gives the normalized capacity as

$$\frac{C_{DCO}}{f_s} = \frac{1}{2} \log_2 \left(1 + \frac{a^2 b^2 T_s}{N_0 R_{LED}} \eta P_{DCO} \right). \tag{9}$$

The modulation index $\alpha(t)$ is usually optimized to maximize η but with sufficiently low clipping noise, not to cause excessive bit errors. In particular, the normalized capacity as in (9) is also called the spectral efficiency.

B. DCO-OFDM IN VLC

The normalized capacity for DCO-OFDM is thus

$$\frac{C_{DCO}}{f_s} = \frac{1}{2} \log_2(1 + SNR_{DCO}) = \frac{1}{2} \log_2(1 + \gamma_{DCO}), \tag{10}$$

where $f_s = 1/T_s$ and (10) is used in later comparisons for VLC.

IV. ACO-OFDM, FLIP-OFDM AND PAM-OFDM

In ACO-OFDM, only the odd subcarriers carry data symbols, while the even subcarriers are set to be zero. The resulting real-valued signal is further clipped, which ensures that the transmitted OFDM signal meets the non-negativity requirement [4]–[7]. The clipping discards half of the original signal power and the remaining part is split evenly among even and odd subcarriers [6].

In Flip-OFDM, a real signal is obtained after IFFT by imposing the Hermitian symmetry property. We can then decompose this signal as $x[k] = x^+[k] + x^-[k]$, where $x^+[k]$ and $x^-[k]$ are the positive and negative parts respectively. These two components are separately transmitted over two successive OFDM symbols [6].

In PAM-OFDM, one-dimension PAM signal is used to modulate the imaginary part of each subcarrier [9], [29]. Similar to ACO-OFDM and Flip-OFDM, Hermitian symmetry applies to the modulated subcarriers in the frequency domain such that the real signal is obtained after IFFT. Then, the signal is also clipped at zero, to ensure positive signal was transmitted over IM/DD channel.

ACO-OFDM, Flip-OFDM and PAM-OFDM signal have the same probability density function (pdf) with a ‘‘clipped Gaussian’’ distribution. Moreover, they result into the same SNR, although the noise power of the Flip-OFDM is doubled during the recombination process of the positive and negative subframes while the signal power is also doubled from the received power.

ACO/Flip/PAM-OFDM signal have a fixed pdf, with a parameter for a different bias strength (mean) and modulation (variance). This implies that for a given LED and current setting, they have only one choice for the power penalty for modulation. This penalty can be substantial. For instance, a Luxeon LED may have $R_{LED} = 1$ Ohm, $I_{LED} = 350$ mA with $V_J = 3.0$ Volt. Illumination power is about $V_J I_{LED} + R_{LED} I_{LED}^2 = 1172$ mW. As we will see later, modulation power is $P_{\Delta FLIP} = (\pi - 1) R_{LED} I_{LED}^2 = (\pi - 1) \cdot 1 \cdot 0.35^2 = 262.3$ mW. So the penalty is 22.4%. In some cases, for instance for energy efficiency certification, this is prohibitively large. Nonetheless all ACO-OFDM, Flip-OFDM and PAM-OFDM can be interesting. Here we analyze the Flip-OFDM, and the results apply to the ACO-OFDM and PAM-OFDM due to the similarity of their statistic properties.

In Flip-OFDM, the signal has a pdf of

$$f(i) = \frac{1}{2} \delta(i) + \frac{U(i)}{\sqrt{2\pi} \sigma_{FLIP}} \exp\left(-\frac{i^2}{2\sigma_{FLIP}^2}\right), \tag{11}$$

where $U(i)$ is the step function and σ_{FLIP} is the standard deviation before clipping the negative part. The expected value of the LED current is

$$\mu_{FLIP} = \frac{1}{2} \sqrt{\frac{2}{\pi}} \sigma_{FLIP} = \sqrt{\frac{1}{2\pi}} \sigma_{FLIP}. \tag{12}$$

The mechanism of the extra power loss in the LED for ACO/Flip/PAM-OFDM is shown in Fig. 3, where we intuitively see that with the same I_{LED} more extra power for ACO/Flip/PAM-OFDM is introduced compared to DCO-OFDM in Fig. 2.

A. ACO-OFDM, FLIP-OFDM AND PAM-OFDM IN IR

For IR, in contrast to previous papers that consider the optical power, we will benchmark based on the total consumed electrical power, including DC bias. In the LED, it consumes

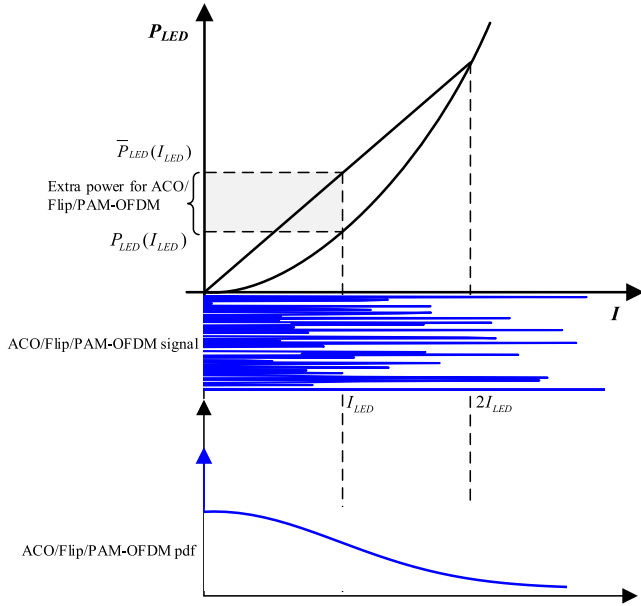


FIGURE 3. Mechanism of the extra power loss in the LED for ACO/Flip/PAM-OFDM, where we assume $\mu_{ACO} = \mu_{FLIP} = \mu_{PAM} = I_{LED}$.

a power of

$$P_{FLIP} = \mathbb{E}[V_{LED}I_{LED}] = V_J \mathbb{E}[I_{LED}] + R_{LED} \mathbb{E}[I_{LED}^2], \quad (13)$$

where, considering that the signal is positive with probability 1/2 we use $\mathbb{E}[I_{LED}] = \sigma_{FLIP}/\sqrt{2\pi}$ and $\mathbb{E}[I_{LED}^2] = \sigma_{FLIP}^2/2$. Thus, the consumed power is

$$P_{FLIP} = \frac{V_J \sigma_{FLIP}}{\sqrt{2\pi}} + \frac{1}{2} R_{LED} \sigma_{FLIP}^2. \quad (14)$$

This allows us to express the capacity in terms of the total consumed power P_{FLIP} . That is, we solve the roots of the above polynomial expression in σ_{FLIP} ,

$$\sigma_{FLIP} = \frac{-\frac{V_J}{\sqrt{2\pi}} \pm \sqrt{\frac{V_J^2}{2\pi} + 2R_{LED}P_{FLIP}}}{R_{LED}}. \quad (15)$$

After recombining the two blocks in Flip-OFDM, the signal has power σ_{FLIP}^2 , while the noise is doubled. Thus this system has the normalized capacity

$$\frac{C_{FLIP}}{T_s} = \frac{1}{2} \log_2 \left[1 + \frac{a^2 b^2 T_s \sigma_{FLIP}^2}{2N_0} \right], \quad (16)$$

where only the positive root in (15) is relevant in this calculation. Note that, in PAM-OFDM, the 0-th and $N/2$ -th subcarriers are usually not modulated with data and thus channel capacity decreases. However, when the number of subcarriers is large, this effect of capacity loss can be neglected.

B. ACO-OFDM, FLIP-OFDM AND PAM-OFDM IN VLC

In VLC, a certain light intensity must be achieved. This dictates the average current through the LED. To achieve the same light intensity as a DCO-OFDM signal, we must

have $\mu_{ACO} = \mu_{FLIP} = \mu_{PAM} = I_{LED}$. Thus, the non-negative OFDM signal must adhere to

$$\sigma_{FLIP} = \sqrt{2\pi} I_{LED}. \quad (17)$$

Thus

$$f(i) = \frac{1}{2} \delta(i) + \frac{U(i)}{2\pi I_{LED}} \exp\left(\frac{i^2}{4\pi I_{LED}^2}\right). \quad (18)$$

The LED consumes a power of

$$\begin{aligned} P_{FLIP} &= \mathbb{E}[V_{LED}I_{LED}] = \int_0^\infty (V_J + R_{LED}i) f(i) di \\ &= V_J I_{LED} + \frac{1}{2} R_{LED} \sigma_{FLIP}^2 \\ &= V_J I_{LED} + \pi R_{LED} I_{LED}^2. \end{aligned} \quad (19)$$

Thus the extra power, above illumination only is

$$P_{\Delta FLIP} = (\pi - 1) R_{LED} I_{LED}^2 = \frac{\pi - 1}{\alpha_{rms}^2} P_{\Delta DCO}, \quad (20)$$

where we can clearly see that for the same I_{LED} , Flip-OFDM consumes more extra power than DCO-OFDM, regardless of the modulation depth ($0 \leq \alpha_{rms} \leq 1$), which confirms the intuition from Fig. 3. Yet, it also gives a better SNR, namely,

$$\begin{aligned} SNR_{FLIP} &= \frac{P_{RX} T_s}{2N_0} = \frac{a^2 b^2 \sigma_{FLIP}^2 T_s}{2N_0} \\ &= \pi \frac{a^2 b^2 T_s}{N_0} I_{LED}^2 = \frac{\pi}{\alpha_{rms}^2} SNR_{DCO}. \end{aligned} \quad (21)$$

Comparing (20) and (21) we conclude that the SNR grows $\pi/(\pi - 1)$ faster than the power consumption. We express the SNR from the extra power for Flip-OFDM, as

$$\gamma_{FLIP} = \pi \frac{a^2 b^2 T_s}{N_0} I_{LED}^2 = \frac{\pi}{\pi - 1} \frac{a^2 b^2 T_s}{N_0 R_{LED}} P_{\Delta FLIP}. \quad (22)$$

Yet, we see that with DCO-OFDM any arbitrary extra power $P_{\Delta DCO}$ can be selected, particularly including small extra powers that fit in typical certified energy-efficient modes. Yet, in Flip and ACO-OFDM, $P_{\Delta FLIP}$ has a fixed relation to the illumination level, and can only work in a regime where the extra power relatively large. A direct comparison between DCO-OFDM and ACO/Flip/PAM-OFDM is complicated by the finding that for VLC no operational point can be found where both schemes have the same DC bias (same illumination level) and the same extra power.

Two ways to overcome the disadvantage that one can only operate ACO/Flip/PAM-OFDM at a full modulation depth are 1) to duty cycle, i.e., to run ACO/Flip/PAM-OFDM in a small percentage of time and to use unmodulated DC bias for the remaining time, and 2) to add a DC bias, in fact we see this as a special case of ADO-OFDM in next section with $\alpha_{rms} = 0$ but $I_{DCO} > 0$.

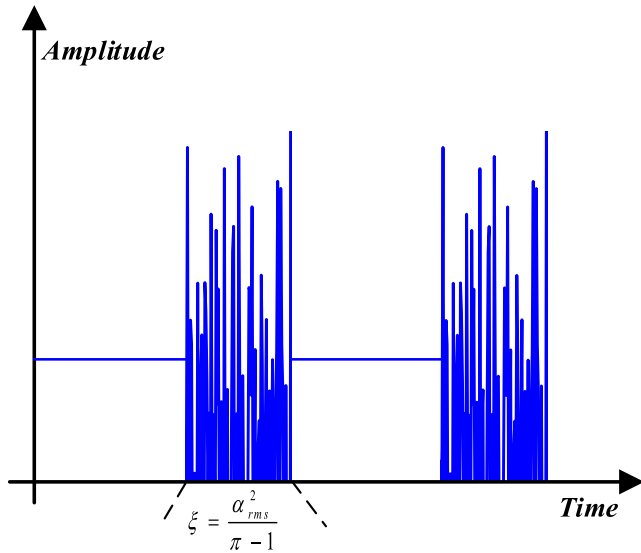


FIGURE 4. ACO/Flip/PAM-OFDM with duty cycling.

C. DUTY CYCLING IN ACO/FLIP/PAM-OFDM VLC

To evaluate in which VLC scenarios ACO or Flip OFDM can be attractive when only a limited *extra* power budget is available, we consider duty cycling. We pose the question whether it is attractive to run a power-efficient clipped OFDM during a fraction of time ξ ($0 \leq \xi \leq 1$), as shown in Fig. 4.

To compare Flip-OFDM and DCO-OFDM for the same illumination level (I_{LED}) and the same extra power P_{Δ} for VLC, the duty cycle ξ must satisfy

$$\xi = \frac{\alpha_{rms}^2}{\pi - 1}. \tag{23}$$

That is, in this regime ACO-OFDM need to run at quite low duty cycles, to avoid that consumes excessive amounts of power. For Flip-OFDM in VLC, we find the normalized capacity as

$$\begin{aligned} \frac{C_{FLIP}}{f_s} &= \frac{\xi}{2} \frac{1}{2} \log_2 \left[1 + \frac{\pi}{\alpha_{rms}^2} SNR_{DCO} \right] \\ &= \frac{\xi}{2} \frac{1}{2} \log_2 \left[1 + \frac{1}{\xi} \frac{\pi}{\pi - 1} \frac{a^2 b^2 T_s}{N_0 R_{LED}} P_{\Delta DCO} \right] \\ &= \frac{\xi}{2} \frac{1}{2} \log_2 \left[1 + \frac{1}{\xi} \frac{\pi}{\pi - 1} \gamma_{DCO} \right]. \end{aligned} \tag{24}$$

We see that for the same I_{LED} , Flip-OFDM does have a larger SNR, as designed for, but the capacity is halved due to the flipping process. Moreover, as reflected in (24) only a fraction of time of ξ contributed. We discuss numerical examples in section VI. We also acknowledge that duty cycling may not be easy to implement, if high light quality without any flicker is demanded. We showed in [14] that during periods of modulation, the light output slightly drops due to convexity and nonlinearities in light output vs current (e.g. droop). So, unless corrected for, the perceived light output may slightly vary with the traffic load ξ , and if on or off periods are longer than a few milliseconds, flicker may be visible.

V. ADO-OFDM AND HACO-OFDM

To mitigate the reduction in spectral efficiency by a factor of 1/2 in ACO/Flip/PAM-OFDM, it has been proposed to include a DC-biased OFDM signal on the orthogonal dimensions, e.g. ADO-OFDM, HACO-OFDM, enhanced U-OFDM (EU-OFDM), spectral and energy efficient OFDM (SEE-OFDM), and Layered ACO-OFDM. This paper analyzes ADO-OFDM and HACO-OFDM. Other variants can be modelled similarly.

A. ADO-OFDM

1) IR SCENARIO

In ADO-OFDM, ACO-OFDM and DCO-OFDM are combined. ACO-OFDM is transmitted over the odd subcarriers and DCO-OFDM is transmitted on the even subcarriers [5], [11]. In particular, an interference cancellation is necessary before the demodulation of the even subcarriers, while odd subcarriers can be demodulated in a similar way as for conventional ACO-OFDM [5], [30].

To calculate the LED power consumption, the pdf of ADO-OFDM signal can be derived by convolving the pdf of ACO-OFDM and that of DCO-OFDM. However, it turns out there is no closed form solution to describe the electrical power [5]. We take the advantage that the ACO-OFDM signal and DCO-OFDM signal for ADO-OFDM are independent and thus the electrical power for each of them can be calculated individually. Considering all contributions, the power consumed in the LED add up to

$$\begin{aligned} P_{ADO} &= \mathbb{E}[V_{LED} I_{LED}] = \int_0^{\infty} (V_J + R_{LED} i) i f(i) di \\ &= V_J \mathbb{E}[I_{LED}] + R_{LED} \mathbb{E}[I_{LED}^2] \\ &= V_J \mathbb{E}[I_{DCO} + I_{ACO}] + R_{LED} \mathbb{E}[(I_{DCO} + I_{ACO})^2] \\ &= V_J \mathbb{E}[I_{DCO}] + V_J \mathbb{E}[I_{ACO}] + R_{LED} \mathbb{E}[I_{DCO}^2] \\ &\quad + 2R_{LED} \mathbb{E}[I_{DCO}] \mathbb{E}[I_{ACO}] + R_{LED} \mathbb{E}[I_{ACO}^2] \\ &= V_J I_{DCO} + \frac{V_J \sigma_{ACO}}{\sqrt{2\pi}} + R_{LED} (1 + \alpha_{rms}^2) I_{DCO}^2 \\ &\quad + 2R_{LED} I_{DCO} \frac{\sigma_{ACO}}{\sqrt{2\pi}} + \frac{R_{LED}}{2} \sigma_{ACO}^2. \end{aligned} \tag{25}$$

The normalized channel capacity of ADO-OFDM is calculated by

$$\begin{aligned} \frac{C_{ADO}}{f_s} &= \frac{1}{2} \frac{1}{2} \log_2 \left(1 + \frac{a^2 b^2}{2N_0 f_s} \alpha_{rms}^2 I_{DCO}^2 \right) \\ &\quad + \frac{1}{2} \frac{1}{2} \log_2 \left[1 + \frac{a^2 b^2}{2N_0 f_s} \sigma_{ACO}^2 \right]. \end{aligned} \tag{26}$$

In particular, we consider the 3-dB noise increment on the DCO-OFDM component of ADO-OFDM caused by the interference cancellation process [5], [30]. Thus a factor of 2 is included in the noise for the capacity calculation for the DCO-OFDM on even subcarriers.

So, for a given power budget P_{ADO} , one can optimize the fraction of power spent on ACO and DCO contributions.

2) VLC SCENARIO

For a constant illumination level I_{LED} , we have the freedom to choose how we split the power, subject to

$$I_{LED} = \mathbb{E}[I_{DCO}] + \mathbb{E}[I_{ACO}] = I_{DCO} + \frac{\sigma_{ACO}}{\sqrt{2\pi}}. \quad (27)$$

For this VLC configuration, the extra power in ADO-OFDM is

$$P_{\Delta ADO} = P_{ADO} - V_J I_{LED} - R_{LED} I_{LED}^2. \quad (28)$$

So, the channel capacity is calculated by

$$\begin{aligned} \frac{C_{ADO}}{f_s} &= \frac{1}{2} \frac{1}{2} \log_2 \left(1 + \frac{a^2 b^2}{2N_0 f_s} \alpha_{rms}^2 I_{DCO}^2 \right) \\ &+ \frac{1}{2} \frac{1}{2} \log_2 \left[1 + \frac{a^2 b^2}{2N_0 f_s} \left[\sqrt{2\pi} (I_{LED} - I_{DCO}) \right]^2 \right]. \end{aligned} \quad (29)$$

B. HACO-OFDM

1) IR SCENARIO

While in HACO-OFDM, ACO-OFDM is transmitted on the odd subcarriers and PAM-OFDM is transmitted on the even subcarriers [9], [11]. Similarly, the power consumed in the LED is

$$\begin{aligned} P_{HACO} &= V_J \mathbb{E}[I_{PAM} + I_{ACO}] \\ &+ R_{LED} \mathbb{E} \left[(I_{PAM} + I_{ACO})^2 \right] \\ &= V_J \mathbb{E}[I_{PAM}] + V_J \mathbb{E}[I_{ACO}] + R_{LED} \mathbb{E} \left[I_{PAM}^2 \right] \\ &+ 2R_{LED} \mathbb{E}[I_{PAM}] \mathbb{E}[I_{ACO}] + R_{LED} \mathbb{E} \left[I_{ACO}^2 \right] \\ &= \frac{V_J (\sigma_{PAM} + \sigma_{ACO})}{\sqrt{2\pi}} \\ &+ R_{LED} \left\{ \frac{1}{2} \sigma_{PAM}^2 + \frac{\sigma_{PAM} \sigma_{ACO}}{\pi} + \frac{1}{2} \sigma_{ACO}^2 \right\}. \end{aligned} \quad (30)$$

The channel capacity of HACO-OFDM is calculated by

$$\begin{aligned} \frac{C_{HACO}}{f_s} &= \frac{1}{2} \frac{1}{2} \frac{1}{2} \log_2 \left[1 + \frac{a^2 b^2}{2N_0 f_s} \sigma_{PAM}^2 \right] \\ &+ \frac{1}{2} \frac{1}{2} \log_2 \left[1 + \frac{a^2 b^2}{2N_0 f_s} \sigma_{ACO}^2 \right]. \end{aligned} \quad (31)$$

Since the interference cancellation process also applies to the demodulation for PAM-OFDM signal [9], the noise level is doubled. However, PAM is modulated on the imaginary part of all the subcarriers in traditional PAM-OFDM while it only occupies the imaginary part of the even subcarriers in HACO-OFDM. Thus, in total, the received SNR is the same in calculating the capacity for PAM-OFDM signal, assuming that σ_{PAM}^2 is the variance before clipping in PAM-OFDM.

2) VLC SCENARIO

For a constant illumination level I_{LED} , we have

$$I_{LED} = \mathbb{E}[I_{PAM}] + \mathbb{E}[I_{ACO}] = \frac{\sigma_{PAM} + \sigma_{ACO}}{\sqrt{2\pi}}. \quad (32)$$

TABLE 1. Parameters for the LED model and VLC channel.

Parameter	Interpretation	Value
V_J	Junction voltage	3.0 Volt
R_{LED}	Dynamic and ESR resistance	1 Ohm
I_{LED}	DC bias current	350 mA
h_0	Optical channel DC gain	3.5×10^{-6}
q	Electron charge	1.6×10^{-19}
R_F	Feedback resistor in RX preamplifier	10^4 Ohm
k	Boltzmann's constant	1.38×10^{-23}
T	Absolute temperature	300 K
a	Responsivity of LED	1 W/A
b	Responsivity of PD	1 A/W
f_s	Equivalent bandwidth	10 MHz

In this VLC configuration, the extra power spent on HACO-OFDM is

$$P_{\Delta HACO} = P_{HACO} - V_J I_{LED} - R_{LED} I_{LED}^2. \quad (33)$$

So the channel capacity is calculated by

$$\begin{aligned} \frac{C_{HACO}}{f_s} &= \frac{1}{2} \frac{1}{2} \frac{1}{2} \log_2 \left[1 + \frac{a^2 b^2}{2N_0 f_s} \sigma_{PAM}^2 \right] \\ &+ \frac{1}{2} \frac{1}{2} \log_2 \left[1 + \frac{a^2 b^2}{2N_0 f_s} \left(\sqrt{2\pi} I_{LED} - \sigma_{PAM} \right)^2 \right]. \end{aligned} \quad (34)$$

VI. PERFORMANCE EVALUATION AND COMPARISON

We assume a preamplifier in the receiver with a feedback resistor of $R_F = 10$ k Ω . As a result, the PSD of the thermal noise is 1.6×10^{-24} A²/Hz. All parameters used in the evaluation and comparison are listed in Table 1. Although the spectrum efficiency only depends on the electrical SNR, the equivalent bandwidth f_s is specified explicitly to calculate the energy efficiency and the noise power in SNR. As a matter of fact, our model and results apply generically and other systems can be evaluated by linear scaling of the curves, accordingly.

A. CAPACITY AND SNR COMPARISON FOR VLC

For equal illumination, I_{LED} , the ratio of Flip-OFDM SNR over DCO-OFDM SNR is π/α_{rms}^2 . For instance, when $\alpha_{rms} = 0.3$, the ratio is 34.9, which however consumes more extra power. For a meaningful comparison of VLC, we set the same extra power budget and same illumination level (I_{LED}), for which we introduced duty cycling. Two extremes give limiting cases.

1) HIGH SNR REGION ($\gamma_{DCO} \gg 2$)

For high SNR, we can approximate Eq. (24) by

$$\frac{C_{FLIP}}{f_s} \approx \frac{1}{2} \frac{\xi}{2} \left[\log_2(\gamma_{DCO}) + \log_2 \left(\frac{\pi}{\pi - 1} \right) - \log_2 \xi \right]. \quad (35)$$

This leads to a capacity bonus of $\log_2 \left(\frac{\pi}{\xi(\pi-1)} \right)$ bits per symbol due to improved SNR (0.553 bits per used dimension more, plus a boost by $\log_2 \xi$). Yet, as every ACO/Flip/PAM-OFDM symbol only partially carries data bits with a

loss of $\xi/2$. Compared with DCO-OFDM using Eq. (10) and (23), we have

$$\begin{aligned} \frac{C_{FLIP}}{C_{DCO}} &= \frac{1}{2\xi} \left[1 + \frac{\log_2(\pi/[\xi(\pi-1)])}{\log_2(\gamma_{DCO})} \right] \\ &= \frac{\alpha_{rms}^2}{2(\pi-1)} \left[1 + \frac{\log_2(\pi/\alpha_{rms}^2)}{\log_2(\gamma_{DCO})} \right], \end{aligned} \quad (36)$$

which is an increasing function with α_{rms} by judging its first-order derivative. Since $0 \leq \alpha_{rms} \leq 0.3$ and $\gamma_{DCO} \gg 2$, we always have $C_{FLIP} < C_{DCO}$. Thus, ACO/Flip/PAM-OFDM is counterproductive for VLC at high SNR.

2) LOW SNR REGION

For low SNR ($\gamma_{DCO} \rightarrow 0$), we can make a series expansion

$$\frac{C_{FLIP}}{f_s} \approx \frac{1}{2} \frac{1}{2} \xi \left(\frac{\pi}{\xi(\pi-1)} \right) \gamma_{DCO}. \quad (37)$$

So, we have

$$\frac{C_{FLIP}}{C_{DCO}} = \frac{1}{2} \left(\frac{\pi}{\pi-1} \right) \approx 0.73, \quad (38)$$

which means ACO/Flip/PAM-OFDM only has 73% of the capacity of DCO-OFDM if we allocate the same mean (illumination) power and the same extra power for communication. Thus, in low SNR region of VLC, one should also not use ACO/Flip/PAM-OFDM.

For low-power IoT data transfer via VLC, one can compare the achievable bit rate given a tiny amount of extra power on top of illumination power. So one can trade-off ACO/Flip/PAM-OFDM with a low duty cycle (occasional) bursts of relatively high rate or DCO-OFDM with a low modulation depth. Typical MAC protocols will anyhow automatically opt for a low duty cycle, which however at the cost of much capacity loss. Fig. 5 shows the large capacity difference for a wider range of SNR, where α_{rms} is swept from 0 to 0.3, for DCO-OFDM, while the corresponding duty cycle ξ that consumes the same extra power ranges from 0 to 4.2%.

To further compare the performance, we consider a commercially available LED. Fig. 6 shows the SNR and channel capacity versus the extra power consumption. The Duty cycling is used to ensure the same average extra power consumption for ACO/Flip/PAM-OFDM, while the SNR is kept constant during the time, i.e., $SNR_{FLIP} = 53.7$ dB. We clearly see that ACO/Flip/PAM-OFDM has larger SNR than DCO-OFDM in this case. In this low extra power regime, DCO-OFDM outperforms ACO/Flip/PAM-OFDM, which has capacity penalty due to duty cycling (very time inefficient), clipping or flipping. On the other hand when we fully exploit ACO/Flip/PAM-OFDM at full duty cycle $\xi = 1$ and average current $I_{LED} = 350$ mA, thus imposing average optical power but not imposing allowing any extra electrical power, a $P_{\Delta ACO/Flip/PAM} = 0.26$ W yields an SNR of 53.7 dB, and delivers 4.46 bis/s/Hz. This is not explicitly shown since $P_{\Delta ACO/Flip/PAM} = 0.26$ W is significantly beyond the x -axis values in Fig. 6 that can be used for DCO-OFDM.

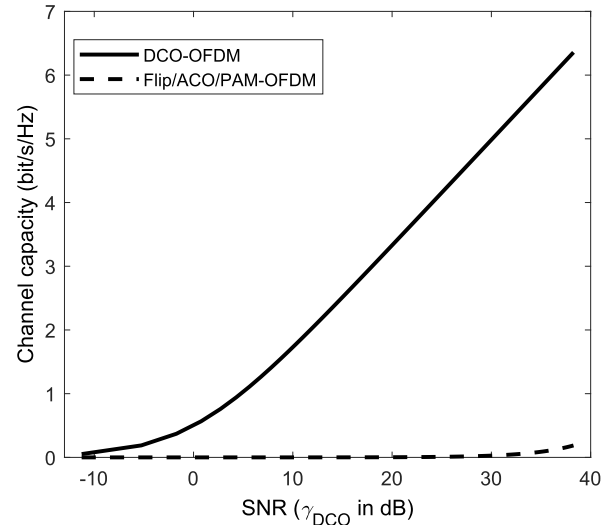


FIGURE 5. Capacity of VLC with a constant illumination ($I_{LED} = 350$ mA) and small extra power for communication. α_{rms} is swept from 0 to 0.3 for DCO-OFDM, accordingly, ξ ranges from 0 to 4.2% for ACO/Flip/PAM-OFDM with same extra power.

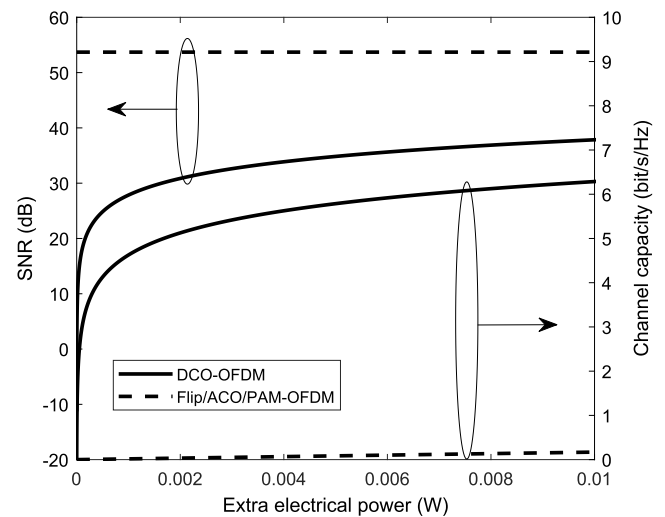


FIGURE 6. Received SNR and channel capacity versus extra electrical power for VLC with a constant illumination ($I_{LED} = 350$ mA). α_{rms} is swept from 0 to 0.3 for DCO-OFDM, accordingly ξ ranges from 0 to 4.2% for ACO/Flip/PAM-OFDM with same extra power.

B. SPECTRAL EFFICIENCY AND ENERGY EFFICIENCY FOR VLC

Fig. 7 shows the spectral efficiency versus energy efficiency for DCO-OFDM, ACO/Flip/PAM-OFDM, ADO-OFDM and HACO-OFDM. All cases have the same illumination level as $I_{LED} = 350$ mA, but not necessarily with the same extra power. As we can see, DCO-OFDM outperforms other schemes in terms of both spectral and energy efficiency.

The detailed performance for ACO/Flip/PAM-OFDM, ADO-OFDM and HACO-OFDM is seen in a subfigure of Fig. 7. By increasing ξ in ACO/Flip/PAM-OFDM, the energy efficiency stays constant, governed by Eqs. (20) and (24). Point A (star) covers a fully loaded ACO/Flip/PAM-OFDM with $\xi = 1$. In Point B only DCO-OFDM (on even

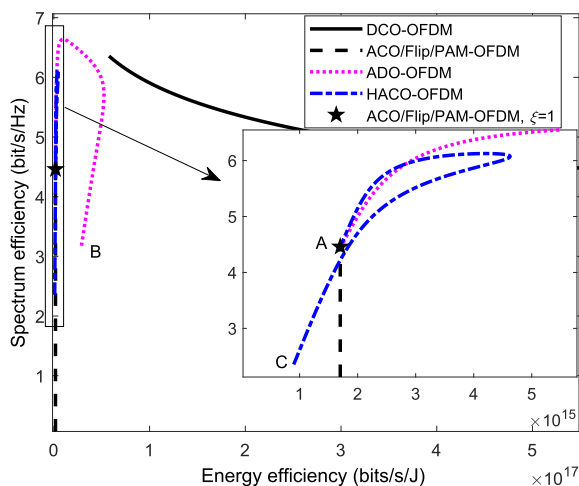


FIGURE 7. Spectral efficiency versus energy efficiency for DCO-OFDM, ACO/Flip/PAM-OFDM, ADO-OFDM and HACO-OFDM, VLC. All cases are configured with $I_{LED} = 350$ mA for a constant illumination level. Point A (star) indicates the unique configuration for ACO/Flip/PAM-OFDM with $\xi = 1$. Point B means only the DCO-OFDM over even subcarriers contributes the communication and illumination in ADO-OFDM, similar to point C but with only PAM-OFDM on even subcarriers in HACO-OFDM.

subcarriers) contributes to communication and illumination in ADO-OFDM. Similarly, point C runs only PAM-OFDM on even subcarriers for HACO-OFDM. As expected, if we only send data over even subcarriers, the spectrum efficiency drops dramatically. Moreover, ADO-OFDM appears more efficient both in spectrally energy-wise than HACO-OFDM. This is understood as DCO-OFDM can carry more information than PAM-OFDM over the even subcarriers.

Fig. 7 indicates that both ADO-OFDM and HACO-OFDM have an optimal efficiency point at a balanced load. A reasonable trade-off is to weight the energy efficiency and spectral efficiency equally, and then find the maximum of their product. Fig. 8 shows the energy efficiency \times spectrum efficiency versus ratio of electrical power on ACO-OFDM subcarriers with a constant illumination. To calculate the power ratio, we particularly use the current ratio of the ACO-OFDM contribution over the average current to split the mixed term of the power consumption in (25) and (30). As we can see, the optimal ratio for ADO-OFDM is 8.5% of the power on the odd subcarriers, while we should spend 53% of the power on odds subcarriers for HACO-OFDM to achieve balanced performance. Moreover, the big performance difference between ADO and HACO-OFDM is mainly due to the inefficient PAM-OFDM signal on even subcarriers in HACO-OFDM, compared to the efficient DCO-OFDM signal in ADO-OFDM. In VLC case with a required current level, we conclude that the traditional PAM-OFDM is inefficient both from spectrum and energy perspective than DCO-OFDM, and thus the combined effect in terms of the product in Fig. 8 for hybrid ADO-OFDM and HACO-OFDM becomes very noticeable.

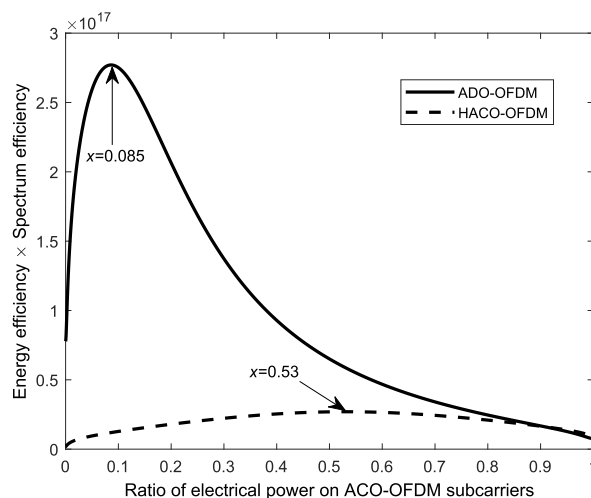


FIGURE 8. Energy efficiency \times Spectrum efficiency versus ratio of electrical power on ACO-OFDM subcarriers for VLC with a constant illumination ($I_{LED} = 350$ mA). The power splitting ratio is the electrical power spent on odd subcarriers with ACO-OFDM to the total power in ADO-OFDM or HACO-OFDM.

C. CAPACITY AND SNR COMPARISON FOR IR

For IR, where any bias only serves to carry the data signal, it is more useful to express the channel capacity as a function of total consumed power, thus including the DC bias power, as in Eqs. (9) and (16). Fig. 9 (left) shows the SNR versus the total consumed power, for the parameters in Table 1. Interestingly, although there is a 3 dB SNR penalty due to the flipping process, Flip-OFDM offers a greater SNR than DCO-OFDM, for a case where they consume the same total power. This agrees with reported simulations work [8], [31]. This improved SNR over DCO-OFDM is not as pronounced for IR (total power) as for VLC (extra power) where a large DC bias is necessary.

The channel capacity versus the total power consumption is shown in Fig. 9 (right). The capacity curves cross each other. In fact, for low signal power, boosting the SNR is more relevant and outweighs the effect that only half the number of dimension is utilized. The latter effect becomes dominant when strong signals are received. We conclude that DCO-OFDM and ACO/Flip/PAM-OFDM each have their own merits, but in very different operational regimes.

D. SPECTRAL EFFICIENCY AND ENERGY EFFICIENCY FOR IR

Fig. 10 shows the spectral efficiency versus energy efficiency for DCO-OFDM and ACO/Flip/PAM-OFDM in IR case. We can see that, DCO-OFDM outperforms ACO/Flip/PAM-OFDM in high SNR region ($>$ around 10 dB). While in low SNR region, ACO/Flip/PAM-OFDM exceeds DCO-OFDM, which further confirms the effect of large capacity for ACO/Flip/PAM-OFDM with low SNR.

Fig. 10 also shows the spectral efficiency versus energy efficiency for ADO-OFDM and HACO-OFDM, where we

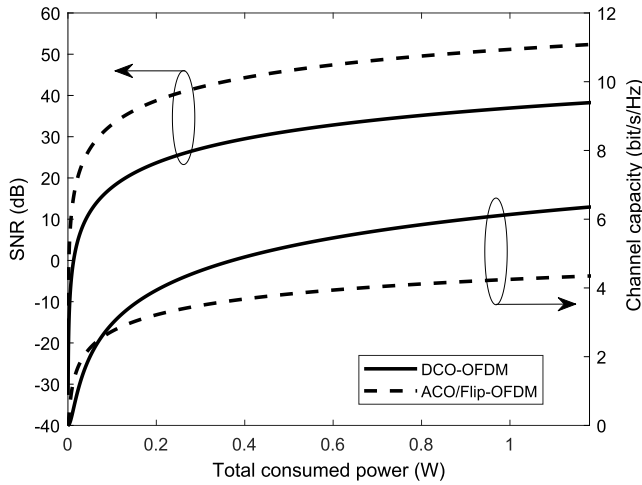


FIGURE 9. Received SNR and channel capacity versus total consumed power for DCO-OFDM and ACO/Flip/PAM-OFDM, IR.

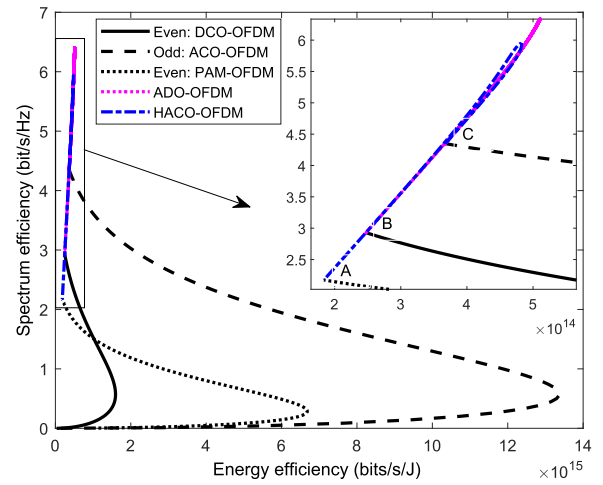


FIGURE 11. Spectral efficiency versus energy efficiency for DCO-OFDM, ACO/Flip/PAM-OFDM, ADO-OFDM and HACO-OFDM, given a power budget for IR.

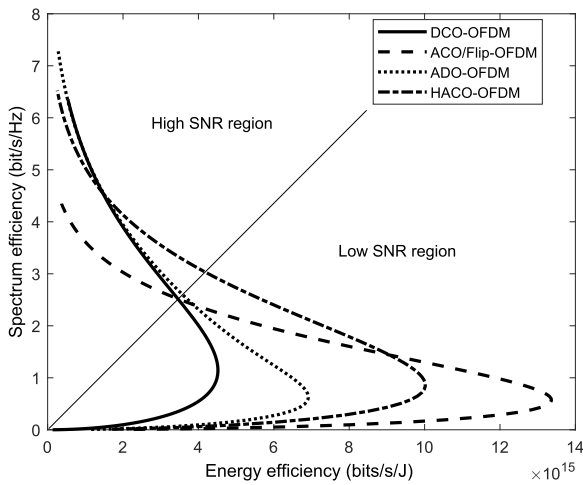


FIGURE 10. Spectral efficiency versus energy efficiency for DCO-OFDM, ACO/Flip/PAM-OFDM, ADO-OFDM and HACO-OFDM, IR. In DCO-OFDM, the bias only serves to carry data, thus we use a bias such that $\alpha_{rms} = 0.3$.

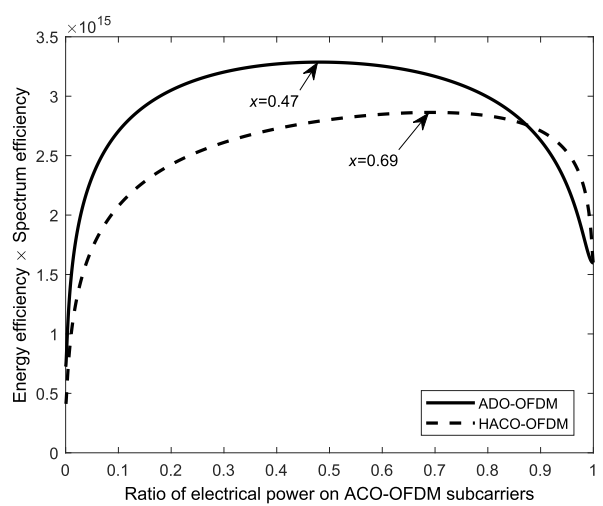


FIGURE 12. Energy efficiency \times Spectrum efficiency versus ratio of electrical power on ACO-OFDM subcarriers, given a power budget for IR. The power splitting ratio is the electrical power spent on odd subcarriers with ACO-OFDM to the total power in ADO-OFDM or HACO-OFDM.

equally assign the same amount of power on odd and even subcarriers. It confirms that ADO-OFDM and HACO-OFDM can improve the energy efficiency in DCO-OFDM and improve the spectrum efficiency in ACO/Flip/PAM-OFDM, to achieve a balanced performance.

However, for a given power budget, one can evenly or asymmetrically split power onto odd and even subcarriers. Fig. 11 shows the spectral efficiency versus energy efficiency for ADO-OFDM and HACO-OFDM, given a power budget for IR. The performance of odd and even subcarriers is also included. In particular, we notice the poorer performance on the subcarriers compared to traditional DCO-OFDM and PAM-OFDM due to practical implementations, for instance the noise increase during interference cancellation process.

In this case, there is no significant energy efficiency improvement in ADO-OFDM and HACO-OFDM, while the spectral efficiency depends on the proportion of power spent on the subcarriers. In fact, for HACO-OFDM signal, point A indicates all the power budget is on even subcarriers

with PAM-OFDM; then the ACO-OFDM on odd subcarriers increases the power consumption, arriving at point C. Similarly, ADO-OFDM starts from point B with only DCO-OFDM on even subcarriers, until to point C with only ACO-OFDM on odd subcarriers. Both ADO-OFDM and HACO-OFDM indicate a optimal power splitting point given a power budget.

To find the optimal trade-off, Fig. 12 shows the energy efficiency \times spectrum efficiency versus ratio of electrical power on ACO-OFDM subcarriers given a power budget. We notice the optimal ratio for ADO-OFDM is 47% of the power on the odd subcarriers and 69% for HACO-OFDM, which is different from VLC case. While similar to VLC, ADO-OFDM and HACO-OFDM have the same performance when the ratio equals 1, since only the odd subcarriers carry data. In particular, VLC is more energy efficient than IR case since the data communication reutilizes parts of the DC power for illumination.

TABLE 2. Comparison summary of DCO-OFDM, ACO/FLIP/PAM-OFDM, ADO-OFDM, and HACO-OFDM.

Parameter	IR								VLC							
	DCO		A/F/P		ADO		HACO		DCO		A/F/P		ADO		HACO	
	L	H	L	H	L	H	L	H	L	H	L	H	L	H	L	H
Energy efficiency	-	+	++	-	+	+	+	+	++	++	-	-	-	-	-	-
Spectrum efficiency	+	++	-	-	+	+	+	+	++	++	-	-	-	-	-	-
PAPR	++	++	-	-	-	-	-	-	++	++	-	-	-	-	-	-
Complexity	++	++	-	-	-	-	-	-	++	++	-	-	-	-	-	-
Nonlinearity tolerance	++	++	-	-	-	-	-	-	++	++	-	-	-	-	-	-
Latency	++	++	-	-	-	-	-	-	++	++	-	-	-	-	-	-

- means worst; - means bad; + means good; ++ means best; L means low SNR; H means high SNR. A/F/P means ACO/Flip/PAM. Except for the low SNR of IR case, we conclude that DCO-OFDM is more efficient than ACO/Flip/PAM-OFDM in terms of both energy and spectrum efficiency.

To this point, the efficiency along with other comparisons for DCO-OFDM and its variants both in VLC and IR case are summarized in Table 2.

VII. CONCLUSION

We witness a continuous effort in improving the energy and spectrum efficiency for basic DCO-OFDM in optimal wireless communications. We confirm that unipolar variants of OFDM outperform DCO-OFDM in low-SNR regions for IR communications. However, when taking into account that a DC bias is required for illumination anyhow, we found that DCO-OFDM is more appropriate than its variants such as ACO/Flip/PAM-OFDM. Even in traditional IR communication where the bias only serves to carry the data signal, DCO-OFDM is still a more appropriate modulation scheme to achieve both high spectrum and energy efficiency in high SNR region. To be specific, ACO/Flip/PAM-OFDM is inefficient if the extra electrical power w.r.t. illumination is used as benchmark. Although a 3 dB penalty is applied in the SNR of ACO/Flip/PAM-OFDM, ACO/Flip/PAM-OFDM offers a greater SNR than DCO-OFDM if they consume the same extra/total power. However the increased SNR still cannot compensate the spectrum inefficiency, resulting into lower overall efficiency compared to DCO-OFDM.

Hybrid ADO-OFDM and HACO-OFDM can achieve a balanced spectrum and energy performance in IR case, but we still notice DCO-OFDM is more energy and spectrum efficient than its variants in VLC where the DC bias is for free. Given a illumination level constraint in VLC and power constraint in IR, there is a different optimal power splitting ratio on odd and even subcarriers in ADO-OFDM and HACO-OFDM. In general, other techniques attempt to achieve the same spectral efficiency as DCO-OFDM by adding several unipolar signals. This increases complexity at the transmitter and the receiver, since several signals are transmitted/received in parallel, requiring several FFTs, etc. In addition, to demodulate the signals interference cancelation is required, which adds noise; one signal is demodulated first and its contribution is subtracted from the received signal before demodulating the rest of the signals, which also increases latency.

REFERENCES

- [1] J. Armstrong, "OFDM for optical communications," *J. Lightw. Technol.*, vol. 27, no. 3, pp. 189–204, Feb. 1, 2009.
- [2] X. Li, J. Vucic, V. Jungnickel, and J. Armstrong, "On the capacity of intensity-modulated direct-detection systems and the information rate of ACO-OFDM for indoor optical wireless applications," *IEEE Trans. Commun.*, vol. 60, no. 3, pp. 799–809, Mar. 2012.
- [3] X. Li, R. Mardling, and J. Armstrong, "Channel capacity of IM/DD optical communication systems and of ACO-OFDM," in *Proc. IEEE Int. Conf. Commun.*, Jun. 2007, pp. 2128–2133.
- [4] J. Armstrong and A. J. Lowery, "Power efficient optical OFDM," *Electron. Lett.*, vol. 42, no. 6, pp. 370–372, Mar. 2006.
- [5] S. D. Dissanayake and J. Armstrong, "Comparison of ACO-OFDM, DCO-OFDM and ADO-OFDM in IM/DD systems," *J. Lightw. Technol.*, vol. 31, no. 7, pp. 1063–1072, Apr. 1, 2013.
- [6] N. Fernando, Y. Hong, and E. Viterbo, "Flip-OFDM for unipolar communication systems," *IEEE Trans. Commun.*, vol. 60, no. 12, pp. 3726–3733, Dec. 2012.
- [7] J. Armstrong and B. J. C. Schmidt, "Comparison of asymmetrically clipped optical OFDM and DC-biased optical OFDM in AWGN," *IEEE Commun. Lett.*, vol. 12, no. 5, pp. 343–345, May 2008.
- [8] A. J. Lowery, "Comparisons of spectrally-enhanced asymmetrically-clipped optical OFDM systems," *Opt. Express*, vol. 24, no. 4, pp. 3950–3966, Feb. 2016.
- [9] B. Ranjha and M. Kavehrad, "Hybrid asymmetrically clipped OFDM-based IM/DD optical wireless system," *IEEE/OSA J. Opt. Commun. Netw.*, vol. 6, no. 4, pp. 387–396, Apr. 2014.
- [10] L. Deng, Y. Rui, P. Cheng, J. Zhang, Q. T. Zhang, and M. Li, "A unified energy efficiency and spectral efficiency tradeoff metric in wireless networks," *IEEE Commun. Lett.*, vol. 17, no. 1, pp. 55–58, Jan. 2013.
- [11] Y. Sun, F. Yang, and L. Cheng, "An overview of OFDM-based visible light communication systems from the perspective of energy efficiency versus spectral efficiency," *IEEE Access*, vol. 6, pp. 60824–60833, 2018.
- [12] A. Jovicic, J. Li, and T. Richardson, "Visible light communication: Opportunities, challenges and the path to market," *IEEE Commun. Mag.*, vol. 51, no. 12, pp. 26–32, Dec. 2013.
- [13] X. Deng, S. Mardankorani, Y. Wu, K. Arulandu, B. Chen, A. M. Khalid, and J.-P. M. G. Linnartz, "Mitigating LED nonlinearity to enhance visible light communications," *IEEE Trans. Commun.*, vol. 66, no. 11, pp. 5593–5607, Nov. 2018.
- [14] X. Deng, Y. Wu, A. M. Khalid, X. Long, and J.-P. M. G. Linnartz, "LED power consumption in joint illumination and communication system," *Opt. Express*, vol. 25, no. 16, pp. 18990–19003, Aug. 2017.
- [15] "Energy star program requirements for lamps (light bulbs), eligibility criteria version 2.1," Tech. Rep., 2017.
- [16] X. Deng, K. Arulandu, Y. Wu, S. Mardankorani, G. Zhou, and J.-P. M. G. Linnartz, "Modeling and analysis of transmitter performance in visible light communications," *IEEE Trans. Veh. Technol.*, vol. 68, no. 3, pp. 2316–2331, Mar. 2019.
- [17] "Advance electrical design led model, application brief AB20-3A," Lumileds, Tech. Rep., 2002.
- [18] J. M. Kahn and J. R. Barry, "Wireless infrared communications," *Proc. IEEE*, vol. 85, no. 2, pp. 265–298, Feb. 1997.
- [19] J. M. Kahn, W. J. Krause, and J. B. Carruthers, "Experimental characterization of non-directed indoor infrared channels," *IEEE Trans. Commun.*, vol. 43, nos. 2–4, pp. 1613–1623, Feb. 1995.
- [20] S. Mardankorani, X. Deng, and J.-P. M. G. Linnartz, "Efficiency of power loading strategies for visible light communication," in *Proc. IEEE Globecom Commun. Workshops (GC Wkshps)*, Dec. 2018, pp. 1–6.

- [21] F. R. Gfeller and U. Bapst, "Wireless in-house data communication via diffuse infrared radiation," *Proc. IEEE*, vol. 67, no. 11, pp. 1474–1486, Nov. 1979.
- [22] H. Yang, J. W. M. Bergmans, T. C. W. Schenk, J. P. M. G. Linnartz, and R. Rietman, "Uniform illumination rendering using an array of LEDs: A signal processing perspective," *IEEE Trans. Signal Process.*, vol. 57, no. 3, pp. 1044–1057, Mar. 2009.
- [23] S. Mardani, A. Alexeev, and J.-P. Linnartz, "Modeling and compensating dynamic nonlinearities in led photon-emission rates to enhance OWC," *Proc. SPIE*, vol. 10940, 2019, Art. no. 109400U.
- [24] J.-P. M. G. Linnartz, L. Feri, H. Yang, S. B. Colak, and T. C. W. Schenk, "Code division-based sensing of illumination contributions in solid-state lighting systems," *IEEE Trans. Signal Process.*, vol. 57, no. 10, pp. 3984–3998, Oct. 2009.
- [25] D. L. Rogers, "Integrated optical receivers using MSM detectors," *J. Lightw. Technol.*, vol. 9, no. 12, pp. 1635–1638, Dec. 1991.
- [26] D. J. F. Barros, S. K. Wilson, and J. M. Kahn, "Comparison of orthogonal frequency-division multiplexing and pulse-amplitude modulation in indoor optical wireless links," *IEEE Trans. Commun.*, vol. 60, no. 1, pp. 153–163, Jan. 2012.
- [27] X. Ling, J. Wang, X. Liang, Z. Ding, and C. Zhao, "Offset and power optimization for DCO-OFDM in visible light communication systems," *IEEE Trans. Signal Process.*, vol. 64, no. 2, pp. 349–363, Jan. 2016.
- [28] J. G. Proakis and M. Salehi, *Digital Communications*, 4th ed. New York, NY, USA: McGraw-Hill, 2001.
- [29] S. C. J. Lee, S. Randel, F. Breyer, and A. M. J. Koonen, "PAM-DMT for intensity-modulated and direct-detection optical communication systems," *IEEE Photon. Technol. Lett.*, vol. 21, no. 23, pp. 1749–1751, Dec. 1, 2009.
- [30] S. D. Dissanayake, K. Panta, and J. Armstrong, "A novel technique to simultaneously transmit ACO-OFDM and DCO-OFDM in IM/DD systems," in *Proc. IEEE GLOBECOM Workshops (GC Wkshps)*, Dec. 2011, pp. 782–786.
- [31] J. Armstrong, B. J. C. Schmidt, D. Kalra, H. A. Suraweera, and A. J. Lowery, "SPC07-4: Performance of asymmetrically clipped optical OFDM in AWGN for an intensity modulated direct detection system," in *Proc. IEEE Global Telecommun. Conf.*, Nov./Dec. 2006, pp. 1–5.



SHOKOUFEH MARDANIKORANI received the B.Sc. degree in electrical engineering from the University of Shahrekord, Shahrekord, Iran, in 2012, and the M.Sc. degree in communication systems engineering from the Sharif University of Technology, Tehran, Iran, in 2014. She is currently pursuing the Ph.D. degree in electrical engineering with the Signal Processing Systems Group, Eindhoven University of Technology, Eindhoven, The Netherlands. Her main research interests include the application of information theory, system modeling and signal processing in optical wireless, and visible light communications.



GUOFU ZHOU received the B.S. degree in metal materials from Chongqing University in China, in 1986, the M.S. degree in materials science from the Institute of Metal Research of Chinese Academy of Science, in 1989, and the Ph.D. degree in materials science from the Institute of Metal Research in China, in 1991 and in Physics from the University of Amsterdam, The Netherlands, in 1994. After more than 20 years working at Philips Research Eindhoven as Principal Scientist, he is currently a Professor of China Talent-1000 Program and the Dean of the South China Academy of Advanced Optoelectronics of South China Normal University. His research interests include optoelectronics materials, devices and systems, with potential applications for displays, smart windows, lighting, and energy.



XIONG DENG (S'13–M'18) received the M.Eng. degree in communication and information engineering from the University of Electronic Science and Technology of China, in 2013, and the Ph.D. degree in optical wireless communications from the Eindhoven University of Technology, Eindhoven, The Netherlands, in 2018. In 2013, he was a Researcher with the Terahertz Science and Technology Research Center, China Academy of Engineering Physics, where he was involved in the integrated terahertz communication and imaging system. He was a Guest Researcher with Signify (Philips Lighting) Research, where he was involved in light fidelity. He is currently a Postdoctoral Researcher with the Eindhoven University of Technology. His research interests include the system modeling, digital signal processing and circuits for intelligent lighting, millimeter wave, radio over fiber, and optical wireless communications.



JEAN-PAUL M. G. LINNARTZ (S'85–M'87–SM'99–F'08) received the M.Sc. degree (*cum laude*) from the Eindhoven University of Technology (TU/e), Eindhoven, The Netherlands, in 1986, and the Ph.D. degree (*cum laude*) from the Delft University of Technology (TU Delft), The Netherlands, in 1991. He was a Senior Director with Philips Research, Eindhoven, where he headed Security, Connectivity, and IC Design Research Groups. He initiated research on Coded Light, to allow the embedding of identifiers in light sources, which is now being used in many office and retail facilities. He is currently a part-time Professor with TU/e, addressing intelligent lighting systems and optical wireless communication, and a Research Fellow with Signify (Philips Lighting) Research. His inventions led to over 60 granted patent families and have been a basis for three successful ventures (Intrinsic-ID, Genkey, and Civolution). In 1993, he introduced multi-carrier CDMA. His papers have been cited more than 10,000 times and his H-index is 51. He is a Fellow of the IEEE for his leadership in Security with Noisy Data. From 1988 to 1991, he was an Assistant Professor with TU Delft. From 1992 to 1995, he was an Assistant Professor with the University of California at Berkeley. In 1994, he was an Associate Professor with TU Delft.

• • •